frontiers | Frontiers in Marine Science

TYPE Original Research
PUBLISHED 01 November 2022
DOI 10.3389/fmars.2022.1030070

OPEN ACCESS

EDITED BY
André Ricardo Araújo Lima,
Center for Marine and Environmental Sciences (MARE), Portugal

REVIEWED BY
Gen Zhang,
Hong Kong University of Science and Technology, Hong Kong SAR, China
Shiguo Li,
Research Center for Eco-environmental Sciences, Chinese Academy of Sciences (CAS), China

*CORRESPONDENCE
Yue Him Wong
timwong@szu.edu.cn
Yu Zhang
biozy@szu.edu.cn

†These authors have contributed equally to this work

SPECIALTY SECTION
This article was submitted to Marine Pollution, a section of the journal Frontiers in Marine Science

RECEIVED 28 August 2022
ACCEPTED 21 September 2022
PUBLISHED 01 November 2022

CITATION
Liang J-Y, Cheng Y-F, Huang X-L, Xu Y, Wong YH and Zhang Y (2022) Behavioral and transcriptomic changes in butenolide treated larvae of the cosmopolitan fouling bryozoan *Bugulina* (*Bugula*) *neritina*. *Front. Mar. Sci.* 9:1030070. doi: 10.3389/fmars.2022.1030070

Behavioral and transcriptomic changes in butenolide treated larvae of the cosmopolitan fouling bryozoan *Bugulina* (*Bugula*) *neritina*

Jin-You Liang[1†], Yi-Fan Cheng[2†], Xiao-Lin Huang[3], Ying Xu[1], Yue Him Wong[2*] and Yu Zhang[1*]

[1]Shenzhen Key Laboratory of Marine Bioresource and Eco-environmental Science, College of Life Sciences and Oceanography, Shenzhen University, Shenzhen, China, [2]Institute for Advance Study, Shenzhen University, Shenzhen, China, [3]Shenzhen Base of South China Sea Fisheries Research Institute, Chinese Academy of Fishery Sciences, Shenzhen, China

The arborescent bryozoan *Bugulina neritina* is a cosmopolitan fouling species in sub-tropical to sub-temperate waters. The butenolide compound 5-octylfuran-2(5H)-one (hereafter named butenolide) reportedly inhibits larval settlement of *B. neritina*, but its effect on the larval behavioral and transcriptomic responses remained unclear. We report that 10 μg mL^{-1} or higher concentration of butenolide and/or prolonged treatment (10 h or longer) resulted in significant increase in larval mortality and prominent spiral larval swimming behavior. The transcriptomic analyses not only revealed up-regulation of typical stress-related protein genes in response to 10 mg mL^{-1} butenolide treatment, but also indicated up-regulation of *mucin*, synaptic genes and nitric oxide signaling genes. In addition, the expression of developmental genes and lipid biosynthesis genes were also affected. Overall, our larval behavior and transcriptome analyses reflected the impact of butenolide on the metabolism, neuronal and molecular signaling in *B. neritina* larvae.

KEYWORDS

butenolide, transcriptome, antifouling (AF), larval swimming behavior, bryozoan *Bugulina neritina*

Introduction

Maritime industries face severe biofouling problem, referring to the undesirable and continuous growth of sessile marine invertebrates on submerged man-made surfaces. Biofouling communities form elaborated structures composed of fouling organisms which could either be soft-foulers, referring to those that have a lightly or non-

calcified body, or hard-foulers, which contain a soft-body protected by a heavily calcified shell (Prevosto et al., 2012).

Marine bryozoans, which form dense colonies by asexual reproduction, are widely distributed worldwide, especially in the Southern Ocean (Marta and Costello, 2020) and are one of the most common foulers (Wood, 2001). Colonies of calcifying species such as those in the genus *Watersipora* grow horizontally and form heavily calcified mats that cover the substratum surface (Brock, 1985; Gordon and Mawatari, 1992). On the other hand, species which adult colonies lack a calcified shell seems to be less problematic, at least to the shipping industry, as these species are neither resistant to high current flow nor salinity changes and are heavily predated (Pratt, 2008). However, these soft bryozoans such as species in the genus *Bugulina* (previously known as *Bugula*) often exhibit strong seasonality. During the growing season, their colonies grow exponentially (Conradi et al., 2000), forming dense bushy colonies. Moreover, certain *Bugulina* species such as *B. neritina* reportedly releases purple color leachates that will chemically induce the larval settlement and subsequent accumulation of the tubeworm *Hydroides elegans* (Bryan et al., 1997; Bryan et al., 1998). As such, the arborescent colonies of soft non-calcified bryozoan species provide a highly elaborate 3D habitat structure and are therefore an important key component in the fouling community (Scheer, 1945; Dumont et al., 2011). For the stake-holders such as fishermen, the growth of soft bryozoans is still highly unwelcome as the bushy colonies often resulted in clogging of fish cages and accumulation of hard foulers (Wood et al., 2013).

Multiple bioactive compounds were found to be inhibitive to the settlement of *B. neritina* larvae, including di(1H-indol-3-yl) methane (DIM) compounds (Wang et al., 2015; Xu et al., 2020) and the butenolide compound 5-octylfuran-2(5H)-one (refers as butenolide hereafter), which was subsequently patented as an antifoulant (Zhang et al., 2011a; Zhang et al., 2012b). The mode of action and toxicology studies raised concern over the commercialization of DIM as an antifoulant, owing to the endocrine disrupting nature of the compound. Butenolide appears to be a promising, non-toxic and environmentally friendly antifoulant. In HeLa cells (Zhang et al., 2011b), marine medaka (*Oryzias melastigma*) (Chen et al., 2014b; Chen et al., 2015), the cypris larvae of the barnacle *Amphibalanus amphitrite* as well as the coronate larvae of *B. neritina*, butenolide mainly affected the gene expression of energy metabolic proteins, especially those associated with or directly involved in lipid or fatty acid metabolism.

For instance, Zhang et al. reported butenolide could bind to very long chain acyl-CoA dehydrogenase (ACADVL), actin, and glutathione S-transferases (GSTs) in *B. neritina* and acetyl-CoA acetyltransferase 1 (ACAT1) in *A. amphitrite* cypris larvae (Zhang et al., 2012b); Chen et al. reported that, in marine medaka, butenolide treatment resulted in increased reactive oxygen species (ROS) production and down-regulation of fatty acid-binding protein, but the effect was concentration dependent and appeared to be transient and reversible when the butenolide concentration was maintained at a low level (Chen et al., 2014a).

Although butenolide was suggested to affect larval energy metabolism, it remains unclear if the compound will trigger severe responses on behavioral and gene expression level. The molecular mode of action of butenolide on marine fouling organism larvae has been examined in multiple model or non-model organisms, including marine medaka (*Oryzias melastigma*) (Chen et al., 2014a; Chen et al., 2015), the cyprid larvae of acorn barnacle *Amphibalanus amphitrite* and bryozoan larvae (Zhang et al., 2011a; Zhang et al., 2012b).

Transcriptomic analyses were typically used to access gene expression changes relating to compound treatment (Heijne et al., 2005; Wu and Wang, 2018). In general, differentially expressed genes (DEGs) between treatment and control groups are identified by bioinformatics and the enriched gene functions among the DEGs are then linked to the compound's effect (Xu et al., 2020). In the case of antifouling compound treatment, highlighted gene functions are generally linked to the inhibitive or inductive effect of the compound on larval settlement. Yet these research efforts focused on the anti-larval settlement effectiveness and the toxicity of the compound. None of these studies reported the immediate short-term effect of the treatment on larval behavior. As the antifouling compound coated on the antifouling paint will constantly release and being diluted by ambient seawater, the amount and duration of larval exposure to the antifouling compound could be highly sporadic.

Application of a chemical compound during the bioassay experiment may lead to acute response such as behavioral changes, including crawling, swimming and phototactic behavior in larvae (Pires and Woollacott, 1997; Shimizu et al., 2000; Zhang et al., 2011a). As gene expression is a highly dynamic process, observing the behavior of larvae in the bioassay experiment is as important as observing the larval settlement rate. We argue that larval behavioral data may provide novel perspectives to the interpretation of transcriptomic data.

In this study, we accessed the effect of the butenolide on *B. neritina* on both behavioral and transcriptomic levels. We firstly observed both larval swimming behavior and the larval settlement rate in *B. neritina* larvae treated with different concentrations of butenolide. Larval behavior was observed by video and the larval swimming track was reconstructed based on video data. Recovery assay was performed to determine the critical concentration and duration of butenolide treatment that caused non-recoverable effect on the larvae. Subsequently, larvae treated with butenolide at the critical concentration and duration, as well as larvae treated with a higher concentration were subjected to RNAseq. Finally, we sought for linkage between the transcriptomic results and behavioral changes.

Materials and methods

Larval settlement assay

Bugulina neritina adult colonies were collected from fishfarm rafts in the Daya Bay, Shenzhen, P. R. China (22°33′53.2″N, 114°32′09.0″E). The adult colonies were kept in dark, transported to the laboratory and maintained in seawater aquarium. To keep the activity of adult colonies, the container was constantly aerated and about one third of seawater was replaced daily. After applying bright light illumination for 30 min to the adult colonies, the released larvae were collected for the settlement bioassays. Butenolide powder was solubilized in 100% DMSO. Before the experiment, butenolide (BU) solutions were prepared in filtrated seawater (FSW) with the final concentrations of 2% DMSO and 2.5, 5, 10, 20, 40 μg mL^{-1} of BU. Five hundred microliters of seawater containing about 10 to 15 larvae were added to each of the well of a 24-well polystyrene plates, followed by the addition of an equal volume of BU solution. In total, seven treatment groups, namely FSW control, 1% DMSO FSW control, 1.25, 2.5, 5, 10 and 20 μg mL^{-1} BU were prepared in quadruplicate. The 24-well plates were kept in dark at room temperature (about 25°C) and the number of settled larvae was recorded after 3 hours using a dissecting microscope (Leica EZ4, Heerbrugg, Switzerland). Larval mortality was recorded at 3, 9, 24 hours. The full set of experiment was repeated three times using three different batches of *B. neritina* larvae released from different adult colonies.

Recovery bioassay

To determine the tolerability and efficacy of the concentration of BU solution during treatment, recovery assays were performed. After adding 20-30 larvae (500 μL in volume) to each well of the 24-well plates, equal volume of BU stock solutions was applied to the final concentration of 1.25, 2.5, 5, 10, 20 μg mL^{-1} with the seawater and DMSO (1%) as control. The plates were placed in dark for 3 hours and then the original solutions were replaced with same volume of fresh seawater twice. The numbers of settled larvae were recorded at 24 hours after incubation in dark.

Larval swimming behavioral analysis

To analyze the effect of BU treatment on larval behavior, three 10 seconds 12 frame per second (fps) video footages were taken using a digital camera (Olympus DP72, Tokyo, Japan) coupled with a stereo microscope (Leica MZ16, Heerbrugg, Switzerland) on each of the six replicates in the control (seawater) group and 5, 10 and 20 μg mL^{-1} BU-treated groups at different time points. For the control group, video footages were taken at 1.5 hours after the initiation of the settlement bioassay; for the 5, 10 and 20 μg mL^{-1} BU-treated groups, video footages were taken at 1.5, 6 hours and 1 hour after recovery from a 3 hours BU treatment. From each video footage, all frames were extracted into.jpeg format image using a python script (provided in Supplementary File 1). The extracted frames were then imported into Adobe Photoshop (version 2020). The initial frame image of a footage was imported firstly as background and all subsequent frame images were adjusted to dim-light mode and then overlaid on top of the initial frame image. Larval swimming behavior was then summarized based on the trajectory of each larva, as visible in the resulting overlaying image of each footage. Larvae with a circular swimming trajectory were concluded as exhibiting looping swimming behavior; larvae that exhibited spiral swimming trajectory were concluded as exhibiting forward looping behavior; larvae swimming trajectory pattern that did not match neither of the above swimming behavior were determined to be typical swimming behavior.

RNAseq sample preparation

Five control larval biological replicate samples, four replicates of 5 μg mL^{-1} and 10 μg mL^{-1} butanolide treated samples were prepared for RNAseq experiment. To prepare RNAseq sample, approximately 300 larvae were treated with 5 or 10 μg mL^{-1} butenolide and the FSW was used as negative control. After incubation in dark for 3 hours, the unsettled larvae were collected for RNAseq analysis, and all samples were frozen with liquid nitrogen immediately and then kept in -80°C until RNA extraction. All treatments were repeated four times.

Total RNA of the larval samples was extracted with TRIzol (Bioer, Hangzhou, China) and the quality of the total RNA was tested using Bioanalyzer (Aglient, Santa Clara, CA, USA). After enrichment and fragmentation of mRNA, cDNA library construction and normalization were conducted using the Illumina Truseq v3 kit according to the standard protocol. The cDNA libraries generated from each sample were sequenced using Illumina HiSeq 2500.

De novo assembling of the transcriptome

All raw read data generated from the RNAseq of five control larval biological replicate samples, four replicates of 5 μg mL^{-1} and 10 μg mL^{-1} butanolide treated samples were deposited to the NCBI Short Read Archive (SRA) with the BioProject accession number PRJNA855486. Clean read data were firstly assembled

using Trinity v2.6.2 (Haas et al., 2013) with the following specific parameters (–min_glue 3 –trimmomatic –max_memory 100G –group_pairs_distance 250 –path_reinforcement_distance 85 –min_kmer_cov 3). The obtained Trinity assembly was further clustered using Corset (Davidson and Oshlack, 2014) based on the result of read mapping and hierarchical clustering of the gene expression pattern of each Trinity transcript (unigene) across all the 12 samples. The clustered assembly was further collapsed at 95% sequence identity using CD-HIT-EST (Li and Godzik, 2006), generating the final *B. neritina* transcriptome assembly.

Annotation and differential expression analysis

The final assembly was then annotated by BLASTx (NCBI-blast+ v.2.10.0) against NCBI non-redundant protein database (nr), NCBI nucleotide database (nt), EuKaryotic Orthologous Groups (KOG), Swiss-Prot, Kyoto Encyclopedia of Genes and Genomes (KEGG) and Gene Ontology (GO). Protein domain assignment was also performed using HMMer against the Pfam HMM database (Finn et al., 2011). E-value cutoff was set as $1e^{-5}$ for homology search by BLASTx and for protein domain assignment by HMMer. In parallel, Illumina read mapping was performed using Bowtie2 (Langmead and Salzberg, 2012) and subsequent transcript abundant estimation was performed using Salmon (Patro et al., 2017). Transcript expression level was normalized to transcripts per million reads (TPM). Differential expression analysis was performed using DESeq2 (Love et al., 2014). Two pairwise comparisons, 5 μg mL^{-1} treatment vs control and 10 μg mL^{-1} treatment vs control, were performed. The threshold for differential expression was set at abs($\log_2$(FoldChange))>1 (or at least 2 times differences) and adjusted p-value < 0.05. The differentially expressed unigenes were selected and further clustered by hierarchical clustering and k-mean clustering. Functional enrichment analysis of KEGG pathway was performed using KOBAS (2.0) (–fdr BH) (Xie et al., 2011), and the threshold for over-representation of a KEGG pathway was set at adjusted p-value < 0.05.

Results

Bioactivity, toxicity and larval recovery tests of BU treatment

At 3 hours post-BU treatment, larval settlement rates at 10 μg mL^{-1} or higher concentrations were significantly lower (ANOVA p<0.001) than the FSW or 1% DMSO FSW control, indicating that BU have a strong and significant inhibitory effect on *B. neritina* larval settlement (Figure 1A), which is in accord with our previous studies (Zhang et al., 2012b). While more than 80% larvae have settled in the control, 1.25 and 2.5 μg mL^{-1} BU treatment groups in the first three hours of the bioassay experiment, persistent inhibitory effect on larval settlement was observed in 10 and 20 μg mL^{-1} BU treatment (Figure 1B). No mortality was observed in all treatment or control groups in the first 3 hours of treatment. However, after 9 hours of BU treatment, more than 74% (± 19%) mortality was observed in 20 μg mL^{-1} BU treatment group (Figure 1C). After 24 hours of BU treatment, all concentrations led to different degrees of larval mortality. Almost all larvae were dead in 10 and 20 μg mL^{-1} BU treatment groups. But in lower BU concentration treatments, only the 5 μg mL^{-1} BU treatment group resulted in significantly higher larval mortality rate than the seawater control group (ANOVA p<0.001) (Figure 1C). The mortality rates at 2.5 μg mL^{-1} and lower BU concentration treatments were not significantly different to the SW or DMSO control group.

In the recovery bioassay, BU solution was replaced by seawater after 3 hours BU treatment and the rate of larvae completed metamorphosis in the recovered wells was observed after 24 hours (3 hours BU+ 21 hours seawater) and compared to that in wells that experienced prolonged 24 hours BU treatment (no recovery). As expected, larvae in the control groups, 1.25 μg mL^{-1} and 2.5 μg mL^{-1} BU treatment groups completed metamorphosis within 24 hours in both the recovery and prolonged BU treatment experiments; larvae in 10 and 20 μg mL^{-1} BU treatment groups could not complete metamorphosis in both the recovery and prolonged BU treatment experiments, suggesting that larvae were unable to recovered from a 3 hours 10 μg mL^{-1} or higher BU concentration treatment; larvae in prolonged 5 μg mL^{-1} BU treatment group could not complete metamorphosis, but removal of BU at 3 hours allowed 87% (± 18%) BU-treated larvae to recover and complete metamorphosis (Figure 1B).

Larval swimming behavioral analysis

To analyze the effect of BU treatment on *B. neritina* larval swimming behavior, we took video footages of *B. neritina* larvae in seawater (SW control), in BU treatments and in recovery experiments (replacement of BU solution with SW). By analyzing the larval movement trajectory, we observed circular looping (see Figure 2A) and spiral swimming behavior (see Figure 2B) among larvae treated with 5 μg mL^{-1} or higher concentrations of BU, but seldom in 1.25 and 2.5 μg mL^{-1} BU-treated or control larvae, which typically exhibited movement with large displacement distances (see Figure 2C).

At 1.5 hours, the percentage of larvae that exhibited circular looping or spiral swimming behavior in 5, 10 and 20 μg mL^{-1} BU treatment (55% ± 12%, 70% ± 20%, 68 ± 10%) groups were significantly higher than in 1.25 and 2.5 μg mL^{-1} BU-treated [3 ± 8% and 4 ± 4%)] larvae and the control groups (SW:2 ± 2%; DMSO 3 ± 5%) (Figure 2D).

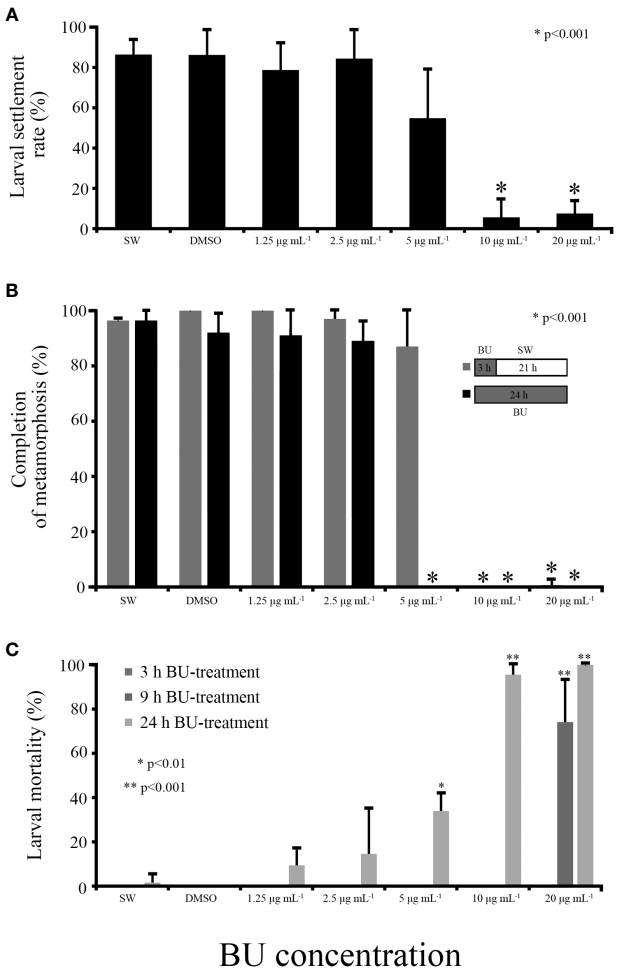

FIGURE 1
Bugulina neritina larval settlement bioassay for butenolide treatment. **(A)** Larval settlement rate after 3 hours of BU treatment. "*" indicates ANOVA p value < 0.001. **(B)** Rate of metamorphosis at 24 hours after the initiation of the bioassay experiment. Larvae in BU treatment groups were treated with BU for 3 hours, after which BU was replaced with autoclaved filtered seawater and incubated for 21 hours in dark until observation. "*" indicates ANOVA p value < 0.001. **(C)** Larval mortality at 3, 9 and 24 hours with different BU concentration treatment. "*" and "**" indicate ANOVA p value <0.01 and < 0.001.

At 6 hours, more than 95% larvae in the control groups (SW and 1% DMSO), 1.25 and 2.5 μg mL^{-1} BU treatment groups already settled and initiated metamorphosis and hence no video was taken for these experimental groups. Similar percentage of unsettled larvae in 5, 10 and 20 μg mL^{-1} BU treatment groups (67% ± 8%, 59% ± 21%, 48 ± 18%) exhibited looping or spiral swimming behavior as at the 1.5 hours time point (Figure 2E).

In the recovery assay, after replacement of BU (after 3 hours treatments) by SW for 1 hour, the percentage of larvae exhibiting looping or spiral swimming behavior in 10 and 20 μg mL^{-1} BU-treated groups (67% ± 8%, 63% ± 9%) remained at a similar level as at 1.5 and 6 hours. In contrast, percentage of larvae exhibited looping or spiral swimming behavior in the recovery assay was significantly lower in the 5 μg mL^{-1} BU treatment group (6 ± 4%) (Figure 2F).

Construction of *Bugulina neritina* transcriptome by RNAseq and *de novo* assembling

Based on the above bioassay results, we define 5 μg mL^{-1} and 10 μg mL^{-1} as "low" and "high" BU concentration (low [BU], high [BU]) treatments. To understand the influence of these BU treatments on larvae, four low and four high [BU] treated larval samples, as well as five untreated "control" larval samples were submitted for cDNA library preparation and HiSeq sequencing. After quality trimming, these 13 samples generated 635,547,702 paired-end reads, composing of 95.33 Gbp. *De novo* assembling of the RNAseq data of all the 13 samples generated a transcriptome assembly containing 138,636 transcripts, which were further clustered into 48,001 unigenes based on the result of

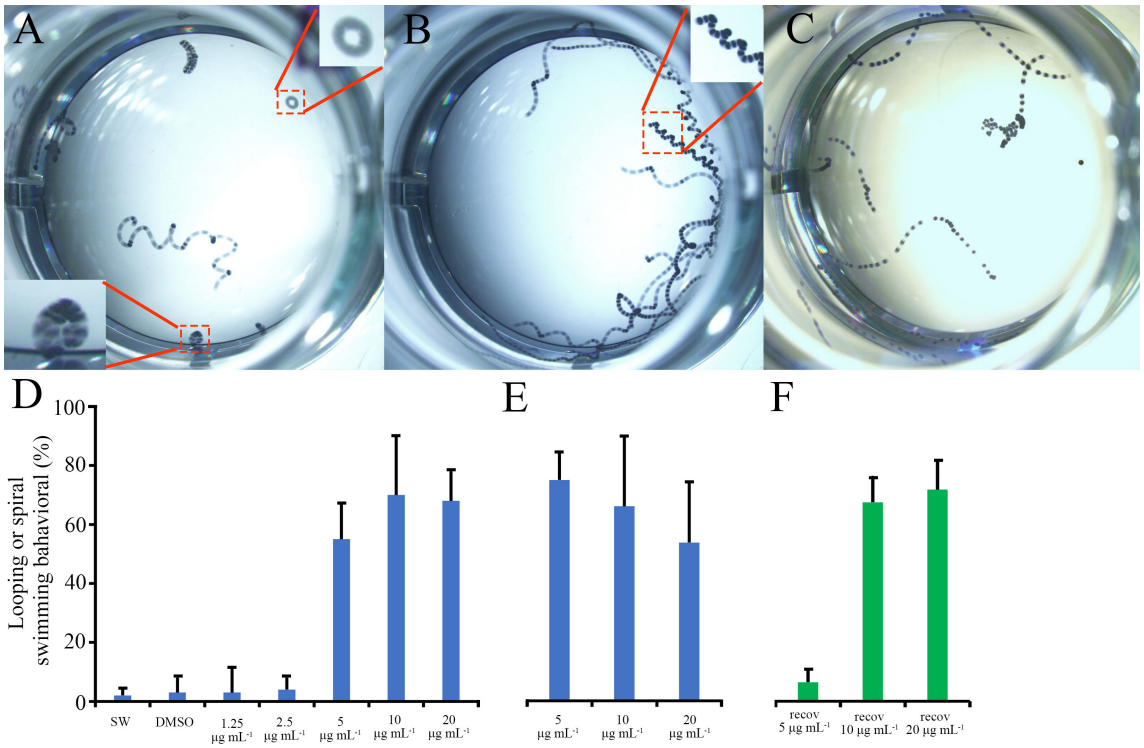

FIGURE 2
Bugulina neritina larval swimming behavior analysis. **(A–C)** Representative overlaid images of all frames of a 10 seconds video which recorded the larval swimming behavior after 1.5 hours of BU treatment. **(A)** Looping swimming behavior of *B. neritina* larvae in 10 μg mL^{-1} BU treatment. **(B)** Spiral swimming trajectory of *B. neritina* larvae in 5 μg mL^{-1} BU treatment. **(C)** The swimming trajectory of *B. neritina* larvae in the control group. **(D, E)** The percentage of larvae exhibiting looping or spiral swimming behavior at **(D)** 1.5 hours and **(E)** 6 hours of BU treatments. **(F)** The percentage of larvae exhibiting looping or spiral swimming behavior at 1 hour after recovery from 3 hours BU treatments in the recovery group.

read mapping and transcript abundance using the Corset algorithm (Davidson and Oshlack, 2014). The transcript length N50 of the assembly is 1,893 bp and the average transcript length is 1,214 bp (Figure S1).

Among the 48,001 unigenes, 22,298 (or 46.45%) were annotated (by BLASTx, e-value cutoff at 1e-5 for homology search, OR, by HMMer for protein domain assignment) by at least one of the public databases, including NCBI nucleotide (nt) sequence database, the NCBI non-redundant (nr) database, SwissProt, Pfam, Gene Ontology (GO), EuKaryotic Orthologous Groups (KOG), KEGG Orthrology (KO) and the KEGG database (Figure S2). Consistent to our previous RNAseq study (Xu et al., 2020), close to 22% of the nr-annotated unigenes were best-matched (share the highest sequence homology) to the brachiopod *Lingula anatina* (Figure S3), once again indicating a potential close phylogenetic relationship between bryozoans and brachiopods, as suggested by an earlier study (Luo et al., 2015).

The functional annotation of the unigenes exhibited different tendency in different functional annotation methods. GO classification of the unigene highlighted the dominance of genes relating to "Binding" and/or "Catalytic activity", in terms of molecular function; "Macromolecule complex", in terms of Cellular Component; "Signaling" and "Regulation of biological process" in terms of Biological Process (Figure S4). On the other hand, KEGG classification indicated the dominance of genes relating to signal transduction and translation (Figure S5).

Differentially expressed genes in response to BU treatment

The transcriptome profiles of high [BU] and low [BU] treated larvae exhibited major differences comparing to the control untreated larvae, as revealed by the Pearson correlation coefficient analysis of the gene expression profile of each sample replicates. However, high [BU] and low [BU] treatments have led to a very similar larval transcriptome profile, as indicated by the outstanding Pearson correlation coefficient (r^2 = 0.845 to

0.911) between high [BU] and low [BU] treated larval samples (Figure S6).

To further characterize the effect of BU on larval gene expression, the larval gene expression levels at high [BU] and low [BU] treatments were compared to that of the control. 8,040 genes were differentially expressed in both high [BU]-to-control and low [BU]-to-control comparisons while only 2,995 were specific to high [BU]-to-control (Figure S7) and 1,757 DEGs to low [BU]-to-control comparisons (Figure S8).

Functional enrichment analysis of differentially expressed genes

To further understand the larval response to BU treatment, the functional enrichment analysis was performed based on the over-representation of enriched KEGG and GO terms among the list of DEG in high [BU]-to-control and low [BU]-to-control comparisons. In the GO enrichment analysis, the GOBP term "DNA integration" and the GOMF term "ATP activity" were both over-represented in both high [BU]- and low [BU]-to-control DEGs (Figures 3A, B), and the fold of enrichment of both GO terms were more significant in the up-regulated DEGs than in the down-regulated DEGs. The GOBP term "xenobiotic metabolic process", which is mainly related to the metabolism of foreign compounds, or in other words, detoxification, was over-represented in the list of up-regulated DEGs in the low [BU]-to-control comparison (Figure 3A).

The list of enriched KEGG terms among the DEG in the low and high [BU]-treated larvae were highly similar. However, the enriched KEGG terms in the up- and down-regulated DEGs were remarkably different. For the up-regulated DEGs, the nervous system related term "Serotonergic synapse", the detoxification related term "ABC transporter", the lipid biosynthesis related term "fatty acid biosynthesis", and the development pathway "Notch signaling pathway" were over-represented (Figures 3C, D); for the down-regulated DEGs, some of the essential functional terms such as "Cell cycle", "Proteasome" and "Ribosome biogenesis in eukaryotes" were over-represented (Figures 3E, F). The results of GO and KEGG enrichment analyses indicated both low and high [BU] treatments suppressed *de novo* synthesis, cell proliferation and developmental processes, and at the same time triggered detoxification and increased energy production.

It is worth to note that *B. neritina* is a non-model organism and some of the differentially expressed genes that have important functions may not be included in the GO or KEGG functional categories. Therefore, we decided to investigate unigenes involved in nitric oxide signaling and other important functional categories that were implicated in larval settlement.

Up-regulation of mucin and serotonergic synapse related genes and the possible linkage with looping swimming behavior

The enrichment of the KEGG term "serotonergic synapse" among up-regulated DEGs in both low and high [BU]-treated larvae suggested the effect of BU treatment on larval nervous system. The list of up-regulated DEGs relating to "serotonergic synapse" included the synaptic enzyme aromatic-L-amino-acid decarboxylase (AADC, or DOPA decarboxylase) which catalyzes the formation of dopamine from L-DOPA, neurotransmitter receptors Gamma-aminobutyric acid receptor (subunit beta) and 5-hydroxytryptamine receptor. The selected list also included a number of intracellular components directly relating to intracellular calcium signaling, including inositol 1,4,5-triphosphate receptor, protein kinase A, phosphatidylinositol phospholipase C and various types of voltage-dependent calcium channels (Tables 1, S1). The above unigenes were up-regulated by 1.2 to 4.3 folds in low and/or high [BU] treated larvae (Table S1).

Up-regulation of NO signaling genes

Five and six nitric oxide synthase (NOS) unigenes were up-regulated in low and high [BU]-treated larvae, with a magnitude of up-regulation ranged from 1.5- to 2.9-fold. In addition to the up-regulation of NOS unigenes, the unigenes encoding downstream components cGMP-dependent protein kinase (PKG), soluble guanylate cyclase (sGC) and guanylate cyclase (GC) were also up-regulated in BU-treated larvae. The soluble guanylate cyclase unigene (Cluster-12452.419) was found to be up-regulated by 1-fold only in low [BU]-treated while the guanylate cyclase unigene (Cluster-13761.0) was up-regulated by 3.5- and 3.1-fold in low and high [BU]-treated larvae; the unigene of PKG was up-regulated by 1.4 and 1.5 fold in low and high [BU]-treated larvae. The expression of the unigene of arginine kinase, which uses the same substrate (L-arginine) as NOS and hence affects one of the upstream components the NO signaling pathway, was not found to exhibit significant variation (data not shown).

Down-regulation of developmental genes

The developmental KEGG term "Notch signaling process" was over-represented among up-regulated DEGs, implying that developmental processes in the larvae were likely to be affected. We therefore investigated in detail the expression pattern of developmental pathway genes. Surprisingly, except *Notch*, which

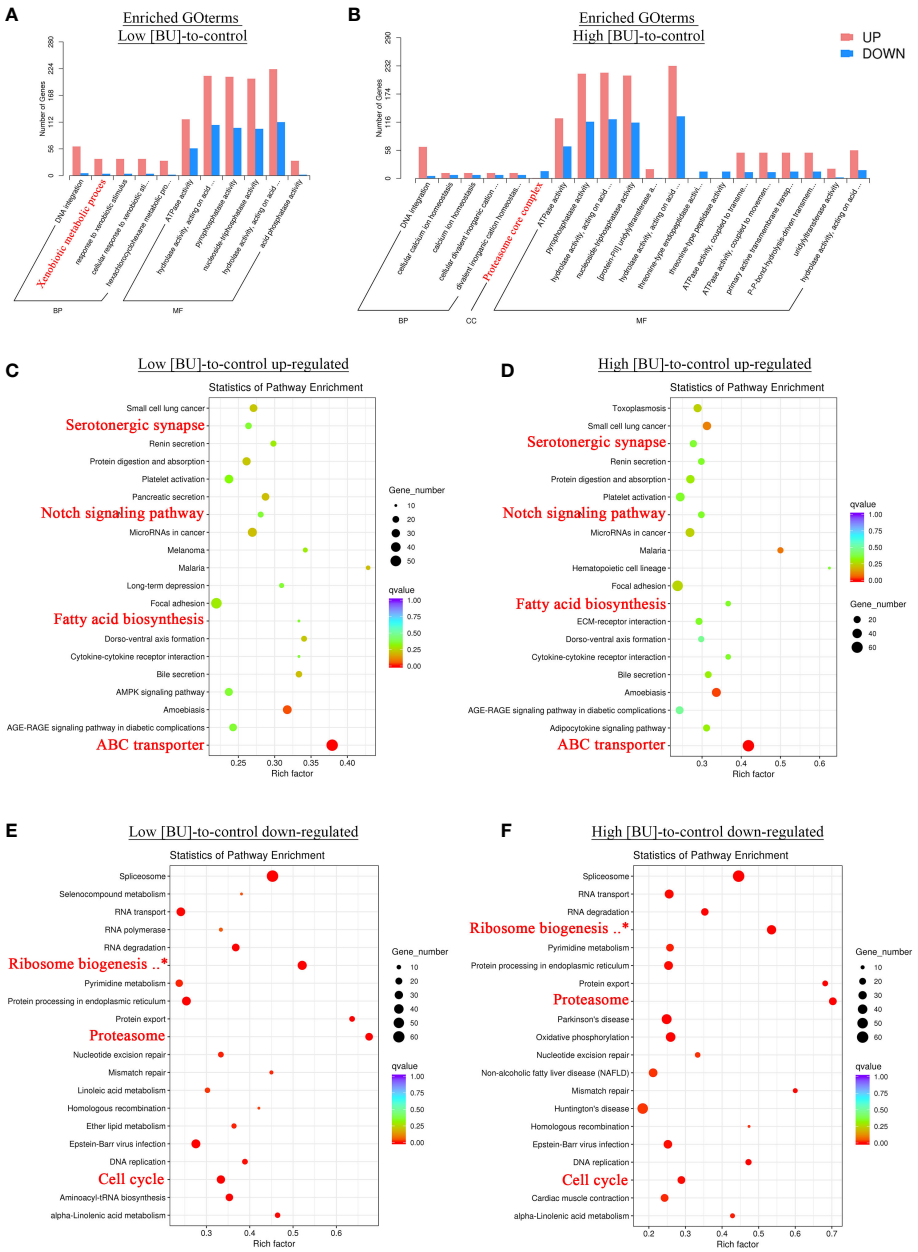

FIGURE 3
GO and KEGG enrichment analyses of differentially expressed genes in response to BU treatment. **(A, B)** Results of GO enrichment analysis. Enriched GO terms among the DEGs in **(A)** low concentration (5 μg mL^{-1}) and **(B)** high concentration (10 μg mL^{-1}) BU treatment were shown. **(C–F)** Results of KEGG enrichment analysis. The enrichment q-values of each enriched KEGG pathway among **(C)** up-regulated and **(D)** down-regulated DEGs in low concentration BU treatment, **(E)** up-regulated and **(D)** down-regulated DEGs in high concentration BU treatment were shown in the dot plots. Pathways that are not relating to human disease and broadly implicated across metazoan taxa were highlighted in red.

was up-regulated by almost two folds in both low and high [BU] treated larvae, other major developmental morphogens were all significantly down-regulated by BU treatment. Wnt ligands *wnt10* (Cluster-12452.10908), *wnt16-like* (Cluster-9233.0), an WNT antagonist *sfrp-5* (Cluster-12452.10592), and the Wnt pathway key player *beta-catenin* (beta-catenin-like protein 1, Cluster-12452.22208) were either not detected in low [BU] or significantly down-regulated in both high [BU] and low [BU] treated larvae. In addition, the BMP ligand *BMP5* (Cluster-12452.1991), the Shh ligand *ihh* (Cluster-12452.18656), were also not detected in low [BU] or significantly down-regulated in the high [BU] treated larvae (Table 1).

TABLE 1 Differentially expressed unigenes in [BU]-treated larvae.

gene_id	nr Description	nr Evalue	LowBU (L)_TPM	HighBU (H)_TPM	Control (C)_TPM	LvsC FoldChange	HvsC FoldChange
Developmental genes							
Cluster-12452.1991	PREDICTED: bone morphogenetic protein 7-like [*Octopus bimaculoides*]	9.00E-46	2.69 ± 0.5	1.96 ± 0.34	3.35 ± 0.46	No diff. exp.	-1.14
Cluster-13882.0	NK1 [*Paracentrotus lividus*]	2.50E-30	1.25 ± 0.32	1.25 ± 0.76	2.43 ± 0.83	-1.04	-1.14
Cluster-12452.10592	soluble frizzled-related protein [*Bugula neritina*]	1.20E-198	55.5 ± 5.6	55.12 ± 2.66	106.43 ± 6.36	-1.17	-1.26
Cluster-12452.18656	sonic hedgehog protein A-like isoform X1 [*Centruroides sculpturatus*]	3.10E-82	1.26 ± 0.13	0.78 ± 0.2	1.96 ± 0.3	No diff. exp.	-1.66
Cluster-9233.0	protein Wnt-16-like [*Centruroides sculpturatus*]	3.2E-75	0.19 ± 0.05	0.13 ± 0.13	1.31 ± 0.14	-2.93	-3.76
Cluster-12452.10908	Wnt protein-like protein 10 [*Bugula neritina*]	2.70E-213	5.6 ± 0.47	5.47 ± 0.91	11.42 ± 0.58	-1.30	-1.42
Cluster-9012.0	PREDICTED: bone morphogenetic protein 2-B [*Crassostrea gigas*]	3.40E-41	0.19 ± 0.09	0.31 ± 0.21	0.38 ± 0.1	-1.29	No diff. exp.
Cluster-12452.22208	beta-catenin-like protein 1 [*Mizuhopecten yessoensis*]	2.00E-101	4.12 ± 1.49	5.06 ± 0.61	7.02 ± 0.67	-1.03	No diff. exp.
Cluster-12452.13130	Notch [*Euperipatoides rowelli*]	0	25.2 ± 4.74	26.88 ± 2.1	5.1 ± 1.25	1.95	1.98
ABC transporter							
Cluster-12452.19959	ATP-binding cassette sub-family A member 3 isoform X1 [*Lingula anatina*]	2.5E-89	11.24 ± 1.11	11.67 ± 1.62	0.33 ± 0.23	4.84	4.88
Unigenes related to serotonergic synapse							
Cluster-12452.29288	tyramine receptor 1 [*Lingula anatina*]	2.4E-15	0.79 ± 0.81	1.41 ± 0.54	0.18 ± 0.12	3.06	2.26
Cluster-14332.0	PREDICTED: aromatic-L-amino-acid decarboxylase-like, partial [*Hyalella azteca*]	1.2E-38	11.21 ± 1.07	11.94 ± 2.48	3.8 ± 1.35	1.29	1.30
Cluster-12452.25929	gamma-aminobutyric acid receptor subunit beta-like [*Lingula anatina*]	2.6E-137	17.65 ± 4.37	18.57 ± 2.64	5.46 ± 0.48	1.44	1.44
Cluster-12452.5288	inositol 1,4,5-trisphosphate receptor [*Lingula anatina*]	2E-54	5.11 ± 2.27	4.2 ± 0.83	0.12 ± 0.14	3.25	3.70
Cluster-12452.21862	phospholipase C beta [*Chaetopterus variopedatus*]	2E-75	7.46 ± 0.99	8.46 ± 1.49	1.03 ± 0.23	2.46	2.37
Cluster-12452.19353	PREDICTED: cAMP-dependent protein kinase catalytic subunit isoform X4 [*Octopus bimaculoides*]	1E-14	1.48 ± 0.55	1.84 ± 0.67	0.6 ± 0.07	1.17	No diff. exp.
Cluster-12452.27039	voltage-dependent calcium channel type A subunit alpha-1 [*Lingula anatina*]	4.5E-200	0.96 ± 0.24	1.43 ± 0.16	0.04 ± 0.04	4.39	3.91
Unigenes related to lipid metabolism							
Cluster-12452.20127	PREDICTED: vitellogenin-1-like isoform X2 [*Saccoglossus kowalevskii*]	2.40E-19	0.69 ± 0.19	0.61 ± 0.12	39.48 ± 2.79	-6.31	-6.03
Cluster-12452.14875	vitellogenin-6 [*Lingula anatina*]	1.80E-09	46.35 ± 31.82	31.85 ± 7.12	3272.55 ± 190.96	-6.91	-6.27
Cluster-12452.15808	vitellogenin-6 [*Lingula anatina*]	1.40E-10	57.58 ± 35.32	36.46 ± 10.02	3801.15 ± 272.71	-6.96	-6.20
Cluster-12452.15767	PREDICTED: vitellogenin-1-like isoform X2 [*Saccoglossus kowalevskii*]	2.60E-11	238.7 ± 104.02	187.26 ± 41.91	9483.73 ± 667.91	-5.97	-5.56
Cluster-12452.14482	fatty acid synthase isoform X1 [*Lingula anatina*]	0.00E + 00	3.69 ± 0.36	7.46 ± 0.5	12.75 ± 0.5	-1.09	-2.03
Cluster-12452.16696	elongation of very long chain fatty acids protein 2-like [*Mizuhopecten yessoensis*]	1.20E-80	4.3 ± 0.36	7.48 ± 1.24	8.7 ± 0.97	No diff. exp.	-1.22
Unigenes related to fatty acid biosynthesis							
Cluster-12452.20752	PREDICTED: LOW QUALITY PROTEIN: long-chain-fatty-acid–CoA ligase 4-like [*Biomphalaria glabrata*]	2.8E-132	31.85 ± 3.99	47.09 ± 5.27	13.52 ± 0.83	1.44	No diff. exp.

(Continued)

TABLE 1 Continued

gene_id	nr Description	nr Evalue	LowBU (L)_TPM	HighBU (H)_TPM	Control (C)_TPM	LvsC FoldChange	HvsC FoldChange
Cluster-12452.8484	acetyl-CoA carboxylase isoform X1 [*Lingula anatina*]	3E-29	13.37 ± 4.22	20.32 ± 4.77	1.61 ± 0.69	3.28	2.86
Unigenes related to nitric oxide signaling							
Cluster-12452.18465	nitric oxide synthase 2, partial [*Bugula neritina*]	2.80E-172	57.64 ± 4.38	63.9 ± 2.39	15.32 ± 3.71	1.66	1.62
Cluster-12452.18466	nitric oxide synthase 2, partial [*Bugula neritina*]	7.40E-226	87.73 ± 7.53	103.12 ± 4.43	16.27 ± 4.96	2.25	2.13
Cluster-12452.18463	nitric oxide synthase 2, partial [*Bugula neritina*]	2.40E-195	38.4 ± 5.92	48.28 ± 1.6	4.93 ± 1.6	2.88	2.67
Cluster-12452.18462	nitric oxide synthase 1, partial [*Bugula neritina*]	1.80E-91	4.36 ± 1.4	3.8 ± 1.01	0.94 ± 0.46	1.21	1.50
Cluster-12452.18464	nitric oxide synthase 1, partial [*Bugula neritina*]	1.50E-124	2.18 ± 0.99	3.31 ± 0.97	0.48 ± 0.28	2.47	1.97
Cluster-12452.18475	nitric oxide synthase 2, partial [*Bugula neritina*]	2.20E-123	64.48 ± 7.36	77.76 ± 1.38	7.19 ± 2.47	2.97	2.81
Cluster-12452.419	soluble guanylate cyclase 88E isoform X4 [*Lingula anatina*]	1.90E-158	2.38 ± 0.37	1.91 ± 0.26	0.94 ± 0.16	No diff. exp.	1.04
Cluster-8666.0	guanylate cyclase 32E [*Lingula anatina*]	7.50E-189	0.68 ± 0.21	0.58 ± 0.27	0.28 ± 0.05	No diff. exp.	1.07
Cluster-13761.0	PREDICTED: guanylate cyclase 32E-like [*Aplysia californica*]	1.30E-59	0.75 ± 0.48	0.62 ± 0.44	0.04 ± 0.04	3.19	3.57
Cluster-12452.29556	cGMP-dependent protein kinase 1 [*Lingula anatina*]	6.80E-52	10.72 ± 2.73	10.14 ± 0.68	2.99 ± 1.01	1.44	1.60

Down-regulation of proteasome genes

Proteasome is one of the over-represented KEGG term in the list of down-regulated DEGs. In fact, there were 29 proteasome DEGs down-regulated in both low and high [BU]-treated larvae and one proteasome DEG down-regulated exclusively in high [BU] treated larvae. These proteasome DEGs were annotated as different subunits, regulatory subunits or non-ATPase regulatory subunit of 20S and 26S proteasomes, proteasomes inhibitor subunits, or proteasome assembly chaperone. The magnitude of down-regulation ranged from 1- to 2.18-fold.

Up-regulation of lipid transporting protein unigenes and down-regulation of vitellogenin genes and genes involve in lipid biosynthesis

Although the KEGG term "fatty acid biosynthesis" was enriched among up-regulated DEGs in both low and high [BU]-treatment groups, it was rather surprising to find that only two lipid metabolic proteins acetyl-CoA carboxylase and long-chain-fatty-acid–CoA ligase were up-regulated. While acetyl-CoA carboxylase catalyzes the production malonyl CoA, the building block for fatty acid biosynthesis, the unigene of fatty acid synthase (Cluster-12452.14482) was down-regulated by 1- and 2-fold in low and high [BU]-treated larvae; the unigene of elongation of very long chain fatty acids protein (Cluster-12452.16696, Cluster-12452.7219) was down-regulated by 1.2-fold in high [BU]-treated larvae; the unigene of fatty acid 2-hydroxylase-like, which is an important lipid metabolic protein in neural tissue, was drastically down-regulated by 5.5- and 5.6-fold in low and high [BU]-treated larvae.

More surprisingly, four vitellogenin-like unigenes were drastically down-regulated in both low and high [BU] treated larvae. The magnitude of down-regulation ranges from 5.6- to 7-fold. These four *B. neritina* vitellogenin-like unigenes were two short sequences (Cluster-12452.14875, Cluster-12452.15808) that were shorter than 500 bp and two long sequences (Cluster-12452.20127, Cluster-12452.15767) that were longer than 4,500 bp. Nevertheless, the deduced ORFs of all four unigenes contained the lipoprotein domain (PF01347) (or Vitellogenin N-terminal domain).

Discussion

Bugulina neritina could settle and metamorphose in as short as 30 min after spawning (Wendt and Woollacott, 1995). The larval nervous system, which links the locomotory coronate ciliated cells, the pyriform organ, the sensory vibration tuft, the eyespots and the adult presumptive tissue internal sac, was

suggested to be the key player in regulating larval settlement (Reed, 1988; Wendt and Woollacott, 1995). For instance, the larval nervous system was suggested to be the key to a coordinated phototactic behavioral response (Reed, 1988). The sensory input from the eye spots and sensory vibration tuft is transduced to the locomotory coronated ciliated cells and the pyriform organ to enable the larvae to perceive and swim toward the light source. Larval contact with the substratum was perceived by the vibration tuft as a mechanical signal and then transduced to the pyriform organ to trigger mucous secretions. Continuous secretion of mucus results in the formation of silk-like thread that stick to the bottom, anchoring the larva to the side or bottom of the well and thereby leading to the cyclic swimming behavior (Young, 2020).

Here, from the video record, we observed BU-treated larvae exhibited spiral or, in certain larvae, concentric swimming behavior. *Bugulina neritina* larvae are phototactic and would swim toward light with a rather direct trajectory. Spiral swimming behavior normally does not occur. Such swimming behavior might indicate failure of the nervous system in coordinating the locomotory organ. Shimizu and colleagues have reported that biogenic amine neurotransmitter, especially serotonin and dopamine, have a major effect on the larval settlement of *B. neritina* (Shimizu et al., 2000). Interestingly, in our gene expression analyses, the KEGG term "Serotonergic synapse" was over-represented and multiple receptors for different neurotransmitters were up-regulated in response to BU treatments. The result overall suggested that the larval nervous system of *B. neritina* might be directly targeted or indirectly affected by BU.

While the spiral swimming behavior might be relating to the nervous system control, the concentric swimming behavior may relate to the pyriform organ mucous secretion. Mucous secretions and anchored swimming larvae can normally be observed during the substratum exploration phase. In fact, the pyriform organ, which is responsible for these secretions, not only contains secretory tissue cells, but is also equipped with a series of specialized sensory cilia (Miyamoto et al., 2013; Wirth et al., 2019). The sticky secretions that form silk-like threads is likely to be released upon mechanical contact with foreign objects and thereby assisting larval attachment at the initial stage. In the laboratory condition, when the larval density was too high and the larvae were too crowded (over 200 larvae in a well of 24-well plate with 2 ml of seawater), the swimming larvae always tended to form a big clump and the larvae in the center of the clump would be trapped within a patch of mucous secretion (unpublished observations). These larval secretions were obviously triggered by mechanical contact between different swimming larvae. However, in our bioassay experiment, the larval density in each well was maintained at 10 larvae per ml of seawater each well. As our transcriptomic analysis indicated that the up-regulation of mucin genes was associated with BU treatment, we propose that BU treatment may not only result in abnormal swimming behavior, but also triggered improper mucus secretion even the larvae were not ready for settlement. As a result, some larvae were anchored to the substratum but at the same time continued to swim vigorously, resulting in the concentric swimming trajectory as observed in the BU bioassay experiment.

NO signal was previously detected in the equatorial nerve ring of *B. neritina* larvae and we have experimentally established that high endogenous or exogenous NO level inhibits larval settlement (Yang et al., 2018b). In addition, the gene expression level of *NOS* and *sGC* or *GC* were all up-regulated during the larval settlement process (Wang et al., 2016; Yang et al., 2018a). As NO in vertebrate systems could act as a neurotransmitter, it was suggested that the inhibitory effect of NO might be mediated through the nervous system (Yang et al., 2018a). Since NOS is the major enzyme producing NO and the enzyme was reportedly expressing in proximity to the equatorial nerve ring (Yang et al., 2018a), BU induced up-regulation of *NOS* gene further suggested the role of nervous system in mediating the inhibitory effect of BU.

Our transcriptomic data also reported the up-regulation of lipid metabolic genes and down-regulation of lipid storage genes. These results, especially the up-regulation of genes encoding acetyl-CoA carboxylase and long-chain-fatty-acid–CoA ligase, are consistent with the finding by Zhang and colleagues that BU targets the energy metabolism of *B. neritina* larvae (Zhang et al., 2012a). However, as we examine the transcriptomic signature of other lipid metabolic genes, it is obvious that there are more down-regulated lipid metabolic and storage genes than up-regulated genes. The result revealed the shortcoming of molecular target identification using chemical pull-down experiments, which lacks a comprehensive view and may lead to mis-conclusion on the effect of the antifouling compound on the larvae.

While BU induced certain behavioral and gene expression changes in *B. neritina* larvae that were previously not reported, the compound did induce consistent down-regulation of proteasome and developmental genes, which were also down-regulated by the treatment of another antifouling compound DIM (Xu et al., 2020). As the chemical structures of BU and DIM differ substantially, they may have very different molecular targets as well as mode of actions. Consistent down-regulation of proteasome and developmental genes may indicate a general larval response to chemical treatment by adjusting its physiology and halting their developmental program. While differential expression of proteasome might be a common stress response, down-regulation of developmental genes including *Wnt10*, *Wnt16*, *Shh*, *sfrp*, *Hox4*, *goosecoid* might be more species specific, as down-regulation of these development genes were not reported in BU-treated barnacle larvae (Zhang et al., 2011a).

The finding that BU and DIM induce the down-regulation of developmental genes has an important environmental implication. Developmental genes typically act as master

regulator in the developmental program across metazoans. For example, the WNT ligands are key morphogens that regulate cellular polarity, axial patterning and cell fate determination. The molecular signal transduction pathway is conserved from sponge to human (Adamska et al., 2010). In *B. neritina*, WNT ligands were suggested to play an important role in the patterning and development of the ancestrula feeding apparatus lophophore (Fuchs et al., 2011; Wong et al., 2012; Wong et al., 2014). For the lecithotrophic larvae of fouling organisms like those of *B. neritina*, which has a very short free-swimming period (as short as 30 min) and which settlement and metamorphosis are simultaneous, the expression of developmental genes should either remains at a low level or be maintained at a constant level during the larval period. Differential expression of these genes may imply that the normal developmental program were likely being disrupted. It is noteworthy, however, that our transcriptomic results reflected the effect of at least 5 μg mL^{-1} BU treatment for at least 3 hours, while in the field, marine larvae may not experience such high concentration and prolonged exposure to the chemical. Nonetheless, we argue that chemicals that induce differential expression of developmental genes deserve special alert to its application. With more compound being tested in the future, we suggest that the gene expression level of developmental genes could be developed into the biomarkers for assessing the degree of impact of antifouling compound on lecithotrophic larvae of marine invertebrates.

In conclusion, we combined behavioral and transcriptomic analyses to acquire a clearer picture on the inhibitory mechanisms of BU on larval settlement. We suggest that BU might not only act on the larval energy metabolism, but could also affect the larval nervous system and mucus secretion in a direct or indirect manner, resulting in the specific looping swimming patterns in *B. neritina* larvae. Besides the specific effect of BU on larval behavior and gene expression, both BU and DIM appeared to trigger down-regulation of developmental genes and up-regulation of proteasome, suggesting important environmental implications on the application of antifouling compounds in the field. Our results once again suggest the commercialization of BU should proceed with cautions.

Data availability statement

The datasets presented in this study can be found in online repositories. The names of the repository/repositories and accession number(s) can be found in the article/Supplementary Material.

Author contributions

Conceptualization: J-YL, Y-FC, YZ, YX and YHW. Data curation: J-YL, Y-FC. Formal analysis: J-YL, Y-FC, YZ, YX and YHW. Funding acquisition: YX, YZ, and YHW. Investigation: J-YL, Y-FC, YX, YZ, and YHW. Methodology: J-YL, Y-FC, YZ, YX and YHW. Project administration: YX, YZ, and YHW. Supervision: YX, YZ, and YHW. Validation: YX, J-YL, YHW. Roles/Writing - original draft: J-YL, Y-FC, YZ, and YHW. Writing - review & editing: J-YL, YX, YZ, and YHW. All authors contributed to the article and approved the submitted version.

Funding

This study was supported grants from Scientific and Technical Innovation Council of Shenzhen and Guangdong Natural Science Foundation (JCYJ20210324093412035 and 2020A1515011117) awarded to YZ; the Innovation Team Project of Universities in Guangdong Province (2020KCXTD023), Natural Science Foundation of Shenzhen University award (2019019) and the Natural Science Foundation of China (41906091) awarded to YHW.

Conflict of interest

The authors declare that the research was conducted in the absence of any commercial or financial relationships that could be construed as a potential conflict of interest.

Publisher's note

Supplementary material

The Supplementary Material for this article can be found online at: https://www.frontiersin.org/articles/10.3389/fmars.2022.1030070/full#supplementary-material

References

Adamska, M., Larroux, C., Adamski, M., Green, K., Lovas, E., Koop, D., et al. (2010). Structure and expression of conserved wnt pathway components in the demosponge *Amphimedon queenslandica*. *Evol. Dev.* 12 (5), 494–518. doi: 10.1111/j.1525-142X.2010.00435.x

Brock, B. J. (1985). South Australian fouling bryozoans. *Bryozoa: Ordovician to Recent*. (Fredensborg, Denmark: Olsen & Olsen), 45–49.

Bryan, P. J., Kreider, J. L., and Qian, P. Y. (1998). Settlement of the serpulid polychaete *Hydroides elegans* (Haswell) on the arborescent bryozoan *Bugula neritina* (L.): Evidence of a chemically mediated relationship. *J. Exp. Mar. Biol. Ecol.* 220 (2), 171–190.

Bryan, P. J., Qian, P. Y., Kreider, J. L., and Chia, F. S. (1997). Induction of larval settlement and metamorphosis by pharmacological and conspecific associated compounds in the serpulid polychaete *Hydroides elegans*. *Mar. Ecol-Prog. Ser.* 146, 81–90. doi: 10.3354/meps146081

Chen, L., Ye, R., Xu, Y., Gao, Z., Au, D. W., and Qian, P. Y. (2014a). Comparative safety of the antifouling compound butenolide and 4,5-dichloro-2-n-octyl-4-isothiazolin-3-one (DCOIT) to the marine medaka (*Oryzias melastigma*). *Aquat. Toxicol.* 149, 116–125. doi: 10.1016/j.aquatox.2014.01.023

Chen, L., Zhang, H., Sun, J., Wong, Y. H., Han, Z., Au, D. W., et al. (2014b). Proteomic changes in brain tissues of marine medaka (*Oryzias melastigma*) after chronic exposure to two antifouling compounds: Butenolide and 4,5-dichloro-2-n-octyl-4-isothiazolin-3-one (DCOIT). *Aquat. Toxicol.* 157, 47–56. doi: 10.1016/j.aquatox.2014.09.010

Chen, L., Sun, J., Zhang, H., Au, D. W., Lam, P. K., Zhang, W., et al. (2015). Hepatic proteomic responses in marine medaka (*Oryzias melastigma*) chronically exposed to antifouling compound butenolide [5-octylfuran-2(5H)-one] or 4,5-dichloro-2-N-octyl-4-isothiazolin-3-one (DCOIT). *Environ. Sci. Technol.* 49 (3), 1851–1859. doi: 10.1021/es5046748

Conradi, M., López-González, P. J., Cervera, J. L., and García-Gómez, J. C. (2000). Seasonality and spatial distribution of peracarids associated with the bryozoan *Bugula neritina* in algeciras bay, Spain. *J. Crustacean Biol.* 20 (2), 334–349. doi: 10.1163/20021975-99990045

Davidson, N. M., and Oshlack, A. (2014). Corset: Enabling differential gene expression analysis for *de novo* assembled transcriptomes. *Genome Biol.* 15 (7), 410. doi: 10.1186/s13059-014-0410-6

Dumont, C. P., Harris, L. G., and Gaymer, C. F. (2011). Anthropogenic structures as a spatial refuge from predation for the invasive bryozoan *Bugula neritina*. *Mar. Ecol-Prog. Ser.* 427, 95–103. doi: 10.3354/meps09040

Finn, R. D., Clements, J., and Eddy, S. R. (2011). HMMER web server: Interactive sequence similarity searching. *Nucleic Acids Res.* 39, W29–W37. doi: 10.1093/nar/gkr367

Fuchs, J., Martindale, M. Q., and Hejnol, A. (2011). Gene expression in bryozoan larvae suggest a fundamental importance of pre-patterned blastemic cells in the bryozoan life-cycle. *Evodevo* 2 (1), 13. doi: 10.1186/2041-9139-2-13

Gordon, D. P., and Mawatari, S. F. (1992). Atlas of marine-fouling bryozoa of new-Zealand ports and harbours. *Miscellaneous Publ. New Z. Oceanographic Institute* 107, 1–52.

Haas, B. J., Papanicolaou, A., Yassour, M., Grabherr, M., Blood, P. D., Bowden, J., et al. (2013). *De novo* transcript sequence reconstruction from RNA-seq using the trinity platform for reference generation and analysis. *Nat. Protoc.* 8 (8), 1494–1512. doi: 10.1038/nprot.2013.084

Heijne, W. H., Kienhuis, A. S., Van Ommen, B., Stierum, R. H., and Groten, J. P. (2005). Systems toxicology: Applications of toxicogenomics, transcriptomics, proteomics and metabolomics in toxicology. *Expert Rev. Proteomics* 2 (5), 767–780. doi: 10.1586/14789450.2.5.767

Langmead, B., and Salzberg, S. L. (2012). Fast gapped-read alignment with bowtie 2. *Nat. Methods* 9 (4), 357–359. doi: 10.1038/nmeth.1923

Li, W., and Godzik, A. (2006). Cd-hit: A fast program for clustering and comparing large sets of protein or nucleotide sequences. *Bioinformatics* 22 (13), 1658–1659. doi: 10.1093/bioinformatics/btl158

Love, M. I., Huber, W., and Anders, S. (2014). Moderated estimation of fold change and dispersion for RNA-seq data with DESeq2. *Genome Biol.* 15 (12), 550. doi: 10.1186/s13059-014-0550-8

Luo, Y. J., Takeuchi, T., Koyanagi, R., Yamada, L., Kanda, M., Khalturina, M., et al. (2015). The *Lingula* genome provides insights into brachiopod evolution and the origin of phosphate biomineralization. *Nat. Commun.* 6, 8301. doi: 10.1038/ncomms9301

Marta, P.-E., and Costello, M. J. (2020). "The biology, ecology and societal importance of marine bryozoa," in *Encyclopedia of the world's biomes*. Eds. M. I. Goldstein and D. A. DellaSala (Oxford: Elsevier), 499–503.

Miyamoto, N., Shinozaki, A., and Fujiwara, Y. (2013). Neuroanatomy of the vestimentiferan tubeworm *Lamellibrachia satsuma* provides insights into the evolution of the polychaete nervous system. *PloS One* 8 (1), e55151. doi: 10.1371/journal.pone.0055151

Patro, R., Duggal, G., Love, M. I., Irizarry, R. A., and Kingsford, C. (2017). Salmon provides fast and bias-aware quantification of transcript expression. *Nat. Methods* 14 (4), 417–419. doi: 10.1038/nmeth.4197

Pires, A., and Woollacott, R. M. (1997). Serotonin and dopamine have opposite effects on phototaxis in larvae of the bryozoan *Bugula neritina*. *Biol. Bull.* 192 (3), 399–409. doi: 10.2307/1542749

Pratt, M. C. (2008). Living where the flow is right: How flow affects feeding in bryozoans. *Integr. Comp. Biol.* 48 (6), 808–822. doi: 10.1093/icb/icn052

Prevosto, M., Davies, P., Compére, C., and Olagnon, M. (2012). "Constraints of the marine environment," in *Marine renewable energy handbook* (Hoboken, New Jersey: Wiley-ISTE) 23–42.

Reed, C. G. (1988). Organization of the nervous system and sensory organs in the larva of the marine bryozoan *Bowerbankia gracilis* (Ctenostomata: Vesiculariidae): Functional significance of the apical disc and pyriform organ. *Acta Zool* 69 (3), 177–194. doi: 10.1111/j.1463-6395.1988.tb00915.x

Scheer, B. T. (1945). The development of marine fouling communities. *Biol. Bull.* 89 (1), 103–121. doi: 10.2307/1538088

Shimizu, K., Hunter, E., and Fusetani, N. (2000). Localisation of biogenic amines in larvae of *Bugula neritina* (Bryozoa: Cheilostomatida) and their effects on settlement. *Mar. Biol.* 136 (1), 1–9. doi: 10.1007/s002270050001

Wang, K. L., Xu, Y., Lu, L., Li, Y., Han, Z., Zhang, J., et al. (2015). Low-toxicity diindol-3-ylmethanes as potent antifouling compounds. *Mar. Biotechnol. (NY)* 17 (5), 624–632. doi: 10.1007/s10126-015-9656-6

Wang, K. L., Zhang, G., Sun, J., Xu, Y., Han, Z., Liu, L. L., et al. (2016). Cochliomycin a inhibits the larval settlement of *Amphibalanus amphitrite* by activating the NO/cGMP pathway. *Biofouling* 32 (1), 35–44. doi: 10.1080/08927014.2015.1121245

Wendt, D. E., and Woollacott, R. M. (1995). Induction of larval settlement by KCl in three species of *Bugula* (Bryozoa). *Invertebr. Biol.* 114 (4), 345–351. doi: 10.2307/3226843

Wirth, M., Wolff, J. O., Appel, E., and Gorb, S. N. (2019). Ultrastructure of spider thread anchorages. *J. Morphol.* 280 (4), 534–543. doi: 10.1002/jmor.20962

Wong, Y. H., Ryu, T., Seridi, L., Ghosheh, Y., Bougouffa, S., Qian, P. Y., et al. (2014). Transcriptome analysis elucidates key developmental components of bryozoan lophophore development. *Sci. Rep.* 4, 6534. doi: 10.1038/srep06534

Wong, Y. H., Wang, H., Ravasi, T., and Qian, P. Y. (2012). Involvement of wnt signaling pathways in the metamorphosis of the bryozoan *Bugula neritina*. *PloS One* 7 (3), e33323. doi: 10.1371/journal.pone.0033323

Wood, T. S. (2001). "14 - bryozoans," in *Ecology and classification of north American freshwater invertebrates (Second edition)*. Eds. J. H. Thorp and A. P. Covich (San Diego: Academic Press), 505–525.

Wood, A. C., Rowden, A. A., Compton, T. J., Gordon, D. P., and Probert, P. K. (2013). Habitat-forming bryozoans in new Zealand: Their known and predicted distribution in relation to broad-scale environmental variables and fishing effort. *PloS One* 8 (9), e75160. doi: 10.1371/journal.pone.0075160

Wu, Y., and Wang, G. (2018). Machine learning based toxicity prediction: From chemical structural description to transcriptome analysis. *Int. J. Mol. Sci.* 19 (8), 2358. doi: 10.3390/ijms19082358

Xie, C., Mao, X., Huang, J., Ding, Y., Wu, J., Dong, S., et al. (2011). KOBAS 2.0: A web server for annotation and identification of enriched pathways and diseases. *Nucleic Acids Res.* 39(Web Server issue), W316–W322. doi: 10.1093/nar/gkr483

Xu, Y., Zhang, L., Wang, K. L., Zhang, Y., and Wong, Y. H. (2020). Transcriptomic analysis of the mode of action of the candidate anti-fouling compound di(1H-indol-3-yl)methane (DIM) on a marine biofouling species, the bryozoan *Bugula neritina*. *Mar. pollut. Bull.* 152, 110904. doi: 10.1016/j.marpolbul.2020.110904

Yang, X. X., Wong, Y. H., Zhang, Y., Zhang, G., and Qian, P. Y. (2018a). Exploring the regulatory role of nitric oxide (NO) and the NO-p38MAPK/cGMP pathway in larval settlement of the bryozoan *Bugula neritina*. *Biofouling* 34 (5), 545–556. doi: 10.1080/08927014.2018.1470240

Yang, X. X., Zhang, Y., Wong, Y. H., and Qian, P. Y. (2018b). HSP90 regulates larval settlement of the bryozoan *Bugula neritina* through the nitric oxide pathway. *J. Exp. Biol.* 221 (Pt 8), jeb167478. doi: 10.1242/jeb.167478

Young, C. M. (2020). "Behavior and locomotion during the dispersal phase of larval life," in *Ecology of marine invertebrate larvae* (Boca Raton: CRC Press), 249–277.

Zhang, Y. F., Wang, G. C., Ying, X., Sougrat, R., and Qian, P. Y. (2011a). The effect of butenolide on behavioral and morphological changes in two marine fouling species, the barnacle *Balanus amphitrite* and the bryozoan *Bugula neritina*. *Biofouling* 27 (5), 467–475. doi: 10.1080/08927014.2011.583985

Zhang, Y. F., Xiao, K., Chandramouli, K. H., Xu, Y., Pan, K., Wang, W. X., et al. (2011b). Acute toxicity of the antifouling compound butenolide in non-target organisms. *PloS One* 6 (8), e23803. doi: 10.1371/journal.pone.0023803

Zhang, Y. F., Kitano, Y., Nogata, Y., Zhang, Y., and Qian, P. Y. (2012a). The mode of action of isocyanide in three aquatic organisms, *Balanus amphitrite*, *Bugula neritina* and *Danio rerio*. *PloS One* 7 (9), e45442. doi: 10.1371/journal.pone.0045442

Zhang, Y. F., Zhang, H., He, L., Liu, C., Xu, Y., and Qian, P. Y. (2012b). Butenolide inhibits marine fouling by altering the primary metabolism of three target organisms. *ACS Chem. Biol.* 7 (6), 1049–1058. doi: 10.1021/cb200545s